Pathophysiology of motor dysfunction in a childhood motor neuron disease caused by mutations in the riboflavin transporter

Manoj P. Menezes [a,b,c,1], Michelle A. Farrar [d,e,f,*,1], Richard Webster [a,c], Jayne Antony [c], Katherine O'Brien [g], Robert Ouvrier [a,b,c], Matthew C. Kiernan [e,h], Joshua Burns [a,i,j,2], Steve Vucic [k,2]

[a] Institute for Neuroscience and Muscle Research, The Children's Hospital at Westmead, Sydney, Australia
[b] Discipline of Paediatrics and Child Health, The Children's Hospital at Westmead Clinical School, The University of Sydney, Sydney, Australia
[c] Department of Neurology, The Children's Hospital at Westmead, Sydney, Australia
[d] Discipline of Paediatrics, School of Women's and Children's Health, UNSW Medicine, The University of New South Wales, Sydney, Australia
[e] Neurosciences Research Australia, Sydney, Australia
[f] Department of Neurology, Sydney Children's Hospital, Sydney, Australia
[g] Department of Audiology, The Children's Hospital at Westmead, Sydney, Australia
[h] Sydney Medical School, Brain & Mind Research Institute, University of Sydney, Sydney, Australia
[i] Paediatric Gait Analysis Service of New South Wales, Sydney Children's Hospitals Network, Sydney, Australia
[j] Sydney Arthritis and Musculoskeletal Research Network, The University of Sydney, Sydney, Australia
[k] Department of Neurology, Westmead Hospital and Western Clinical School, University of Sydney, Sydney, Australia

ARTICLE INFO

HIGHLIGHTS

- Nerve excitability studies in Brown–Vialetto–Van Laere syndrome due to RFVT2 deficiency suggest that an increase in myelin permeability underlies the motor nerve dysfunction.
- These abnormalities are partially reversed by riboflavin therapy.
- Nerve excitability studies may be further developed in larger cohorts as a potential biomarker to identify treatment response.

ABSTRACT

Objective: Brown–Vialetto–Van Laere (BVVL) syndrome is a progressive motor and sensory neuronopathy secondary to mutations in *SLC52A2* encoding the riboflavin transporter type 2 (RFVT2). The phenotype is characterized by early childhood onset hearing loss and sensory ataxia followed by progressive upper limb weakness, optic atrophy, bulbar weakness and respiratory failure. To gain further insight into disease pathophysiology and response to riboflavin supplementation, the present study investigated whether axonal ion channel or membrane abnormalities were a feature of BVVL.
Methods: Axonal excitability studies and clinical assessments were prospectively undertaken on six patients with BVVL secondary to riboflavin transporter deficiency type 2 (age range 10–21 years) at baseline and after 12 months of riboflavin (1000 mg daily) therapy.
Results: At baseline, depolarizing and hyperpolarizing threshold electrotonus was 'fanned out' and superexcitability was increased, while the resting current–threshold gradient and refractoriness were significantly reduced in BVVL patients when compared to controls. Mathematical modeling suggested that functional alterations of myelin underlay these findings with an increase in myelin permeability. Riboflavin therapy resulted in partial normalization of the axonal excitability findings, paralleled by maintenance of muscle strength.
Conclusions: The present study established that abnormalities in myelin permeability at the paranode was a feature of BVVL and were partially normalized with riboflavin therapy.

* Corresponding author at: Department of Neurology, Sydney Children's Hospital, High St., Randwick, NSW 2031, Australia. Tel.: +61 2 93821549; fax: +61 2 93821580.
   E-mail address: m.farrar@unsw.edu.au (M.A. Farrar).
   [1] These authors contributed equally to this work.
   [2] These senior authors contributed equally to this work.

Significance: This study reveals a novel pathophysiological process for motor nerve dysfunction in BVVL. It also indicates that nerve excitability studies may be further developed in larger cohorts as a potential biomarker to identify treatment response for BVVL patients.

1. Introduction

Brown–Vialetto–Van Laere (BVVL) syndrome is a progressive neurodegenerative disorder characterised by pontobulbar palsy and sensorineural hearing loss (Sathasivam, 2008). Recently, a significant number of patients with BVVL have been shown to harbor homozygous or compound heterozygous mutations in *SLC52A2* and *SLC52A3* (Green et al., 2010; Johnson et al., 2012). The *SLC52A1, -A2* and *-A3* genes, encoding the riboflavin transporters RFVT1, RFVT2 and RFVT3, are members of the solute carrier family 52 and are localized within the cytoplasm and endosomal vesicles. While the riboflavin transporters RFVT1 and RFVT3 are highly expressed in the small intestine, RFVT2 expression is most pronounced in fetal brain and spinal cord (Yao et al., 2010). Patients with RFVT2 deficiency develop a motor and sensory neuronopathy clinically characterized by childhood-onset pontobulbar palsy, sensory ataxia, upper limb weakness and respiratory insufficiency, together with sensorineural deafness and optic atrophy (Johnson et al., 2012). This rare neurodegenerative disorder has a poor prognosis, resulting in loss of ambulation, respiratory failure requiring ventilation and early death (Foley et al., 2014).

Functional studies have demonstrated that RFVT2 mutations reduced both riboflavin uptake and riboflavin transporter expression (Haack et al., 2012; Foley et al., 2014). Riboflavin is critical for the biosynthesis of flavin mononucleotide (FMN) and flavin adenine dinucleotide (FAD), important cofactors for carbohydrate, amino acid and lipid metabolism. FAD acts as an electron acceptor in acyl-CoA dehydrogenase reactions in mitochondrial fatty acid oxidation and branched chain amino acid catabolism. Untreated patients with BVVL exhibit an increase in the levels of serum medium-chain acylcarnitines, which normalize rapidly after riboflavin supplementation. In addition, supplementation with riboflavin may exert a neuroprotective benefit by slowing the disease course and improving motor function (Bosch et al., 2011; Johnson et al., 2012; Foley et al., 2014). While identification of mutations in the riboflavin transporters have opened the way to therapy for BVVL, the pathophysiological basis of motor neuron dysfunction in this condition remains unclear.

The development of sensory and motor neuronopathy is a common clinical feature of BVVL. Nerve conduction studies in BVVL due to RFVT2 deficiency reveal a severe axonal sensory neuronopathy at presentation, followed by the development of a progressive motor neuronopathy (Foley et al., 2014). Pathological studies in BVVL have disclosed degeneration of sensory and motor neurons, in keeping with the neurophysiological findings (Francis et al., 1993; Foley et al., 2014). Novel neurophysiological tools, such as axonal excitability, could provide unique pathophysiological insights in BVVL. Importantly, the axonal excitability techniques have been applied in related neurodegenerative disorders, such as motor neuron disease, and have identified significant abnormalities in axonal ion channel function (Kiernan et al., 2000; Vucic and Kiernan, 2006, 2007a,b; Farrar et al., 2011). Consequently, the aim of the present study was to use these axonal excitability tests to better characterize the pathophysiological basis of motor axon dysfunction in BVVL, and the extent to which any identifiable abnormalities of axonal excitability might respond to treatment with riboflavin.

2. Subjects and methods

Patients with BVVL due to mutations in the *SLC52A2* gene were prospectively recruited from a specialized neuropathy clinic. Henceforth, the term BVVL will be used for this group. Clinical (grip strength), functional (respiratory function testing and audiometry), and biochemical (acylcarnitine profile) assessments were combined with conventional and specialized neurophysiological tests. Informed consent or assent was obtained from all participants and the study was approved by the South Eastern Sydney and Illawarra Area Health Service and The Children's Hospital at Westmead Human Research Ethics Committees. Assessments were undertaken at baseline, at the time of initiation of riboflavin treatment, and after 12 months of treatment. All patients were treated with 1000 mg/day of oral riboflavin (Herbs of Gold, Riboflavin 200 mg tablets, Kirrawee, Australia), equating to a dose on 20–26 mg/kg/day.

2.1. Nerve excitability studies

Nerve excitability studies were undertaken corresponding to a previously described protocol (Kiernan et al., 2000). Stimulus current was delivered at the wrist to the median nerve, recording over the abductor pollicis brevis muscle (APB). Skin temperature was at or above 32 °C at the site of stimulation. The TRONDNF protocol of the multiple nerve excitability QTRACs software was used for the studies (Institute of Neurology, London, England).

Multiple excitability measures were assessed, incorporating: stimulus response curves, strength–duration properties, threshold electrotonus (TE), current–threshold relationship (*IV*), and recovery cycle (see Section 6). The stimulus strength necessary to excite nerves as stimulus width was increased from 0.2 to 1 ms duration was determined to describe strength–duration properties, including calculation of strength duration time constant (T_{SD}) and rheobase (Bostock et al., 1998). Threshold electrotonus used sustained 100 ms sub threshold currents fixed at ±40% of the control threshold current (depolarizing, TEd and hyperpolarizing, TEh) to modify the potential difference through the internodal membrane of the axon. Threshold was assessed before, during and after the conditioning currents at 26 various times, for example, TEd 10–20 denotes the decrease in threshold for depolarizing threshold electrotonus at the 10–20 ms interval. *IV* relationship described axonal rectifying properties and utilized polarizing currents of 200 ms duration, altering their strength from +50% (depolarizing) to −100% (hyperpolarizing) of the control threshold (Bostock et al., 1998). The resting *I/V* slope was determined from polarizing currents +10% to −10%. The recovery cycle measured alterations in threshold following a supramaximal conditioning stimulus at various conditioning-test intervals reducing from 200 to 2 ms, and included a refractory period at brief conditioning-test intervals, followed by a phase of superexcitability and then late subexcitability (Kiernan et al., 1996).

2.2. Mathematical model of nerve excitability

To evaluate the probable biophysical basis of the nerve excitability changes in patients with BVVL, mathematical

simulations using a model of the human axon were performed with the MEMFIT software contained within QtracP data analysis programme (Bostock et al., 1991; Farrar et al., 2011). This utilizes an iterative least squares method to minimize the difference between simulated excitability parameters and the recorded patient excitability measures.

2.3. Statistical analysis

Measurements between BVVL patients at baseline were compared to the 95% confidence intervals (CI) of healthy controls (and considered significant if outside this range). Control data was obtained from 17 age-matched participants (9 males, 8 females; age range 9–18 years, mean 12.4 years). Paired Student *t*-tests were used to determine differences between BVVL patients before and after treatment. A *p*-value of <0.05 was considered statistically significant. Results in BVVL patients are expressed as mean ± standard error of the mean (SEM) and in healthy controls as mean and 95% confidence intervals (CI).

3. Results

3.1. Clinical features

A total of 6 patients, aged between 10 and 21 years, from 3 different families (patients 1.1 and 1.2 from family 1, 2.1 from family 2, and 3.1, 3.2 and 3.3 from family 3) were recruited for this study (Table 1). All patients were homozygous for the p.G306R mutation in SLC52A2, except for patient 2.1 who had compound heterozygous p.G306R/p.L339P genotype. The clinical phenotype in the current cohort was typical for BVVL and characterized by sensory ataxia, progressive upper limb, axial and respiratory weakness along with cranial neuropathy affecting cranial nerves II (optic atrophy) and VIII (sensorineural hearing loss) (Foley et al., 2014). Hearing deteriorated rapidly, with patients progressing from normal to lip-reading within 2 years. Upper limb weakness and wasting was not present at onset, but rapidly developed during childhood, and was ultimately severe, resulting in a flail-arm phenotype. Bulbar symptoms included dysarthria, tongue weakness and dysphagia. Respiratory weakness requiring invasive or non-invasive respiratory support was present in 2 patients. Cognition was preserved in all patients.

3.2. Baseline nerve excitability

Conventional neurophysiological testing disclosed the presence of an axonal sensorimotor polyneuropathy in subjects with BVVL (Table 1). Nerve excitability was assessed in three patients with recordable median CMAP responses (patients 1.1, 1.2 and 3.3) 2, 6 and 16 years after symptom onset respectively. The other three subjects exhibited absent or significantly reduced median motor responses, such that axonal excitability studies could not be undertaken on these patients. In the tested group, the CMAP amplitude was similar to healthy controls (BVVL, 5.4 ± 1.2 mV; controls, 6.3 mV [95% CI 4.1–8.4]). The threshold currents required to elicit a response were similar in BVVL patients and controls (BVVL, 2.6 ± 1.2 mA; controls, 3.2 mA [95% CI 1.2–5.2]). The strength duration time constant (BVVL, 0.42 ± 0.03 ms; controls, 0.40 ms [95% CI

Table 1
Comparison of assessments in patients with BVVL at baseline and after 12 months of riboflavin therapy.

	1.1		1.2		2.1		3.1		3.2		3.3[*]	
Gender	F		F		F		M		M		M	
Disease duration (y)	2		6		10		13		13		16	
	Baseline	1 year	Baseline	1 year	Baseline	1 year	Baseline	1 year	Baseline	1 year	Baseline	1 year
Age at assessment (years)	10	11	9	10	15	16	16	17	16	17		21
Grip (Newtons)	118	174	72	82	0.7	0	20	24	0	36		326.7
Audiometry												
Pure tone audiometry	Bilateral mild low-frequency	Normal	R – moderate-severe, L – severe-profound	R – mild-moderate, L – severe rising to moderate	Bilateral moderate-severe	Bilateral moderate-severe	Bilateral profound	Bilateral profound	Bilateral profound	Bilateral profound		Bilateral profound
Respiratory function testing (% predicted)	(at 6 months of therapy)				(6 months of therapy)		Ventilated		BiPAP			
FVC	95	93	ND	97	66	68						77
BiPAP/ventilation pressure (cm of H2O)							16/5	12/5	20/8	18/8		
Nerve conduction studies												
Median motor (APB)												
CMAP (mV)	9.3	6	**3.1**	4.2	**NR**	**NR**	**NR**	**NR**	**NR**	1.4	7	6
DML (ms)	3.4	3.4	3.6	3.7						3.9	3.4	3.5
CV (m/s)	49	**47**	**43**	49						**41**		
Tibial motor (AH)												
CMAP (mV)	8	9.8	6.3	4.3	13.2	13.1	9.6	8.3	10.4	11.9		
DML (ms)	3.9	5.6	3.9	3.2	3.6	3.5	4.7	3.6	4.9	4.7		
CV (m/s)	45	47	42	45	40	42	44	44	38	41		
Median SAP (μV)	**NR**	**NR**	**NR**	**NR**	5	3	**NR**	**NR**	**NR**	**NR**		
Sural SAP (μV)	**NR**	**NR**	**NR**	**NR**	**NR**	**NR**	**NR**	**NR**	**NR**	**NR**		
Acylcarnitine profile	Abnormal[a]	Normal	Abnormal[a]	Normal	Abnormal[a]	Normal	Normal	Normal	Normal	Normal		Normal

M, male; F, female; CMAP, compound muscle action potential; SAP, sensory action potential; NR, not recordable; ND, not done; L, left; R, right; FAD, flavin adenine dinucleotide. Normal values for nerve conduction studies from Preston and Shapiro (2012). Abnormal nerve conduction study results in bold.

[a] Elevated medium chain acylcarnitines.
[*] Baseline data not available.

Table 2
Results of motor nerve excitability testing.

	Normal n = 17	BVVL baseline n = 3	BVVL on riboflavin n = 3
CMAP amplitude	6.3 [4.1–8.5]	5.4 ± 1.2	5.1 ± 1.1
Strength duration time constant (ms)	0.40 [0.36–0.44]	0.42 ± 0.03	0.41 ± 0.02
Threshold electrotonus			
Depolarizing TE peak (%)	65.1 [62.6–67.7]	76.2 ± 0.4	76.2 ± 2.6
Depolarizing TE 40–60 ms (%)	50.6 [48.6–52.6]	61.5 ± 0.3	58.4 ± 1.7
Depolarizing TE 90–100 ms (%)	**42.6 [40.6–44.6]**	**56.1 ± 2.3**	**49.3 ± 1.3**[†]
Hyperpolarizing TE 10–20 ms (%)	**−70.8 [−74.5 to −67.1]**	**−88.8 ± 4.6**	**−77.9 ± 1.9**[†]
Hyperpolarizing TE 90–100 ms (%)	**−107.8 [−116.6 to −99]**	**−151.7 ± 10.2**	**−129.9 ± 5.5**[†]
Current–voltage relationship			
Resting I/V slope	0.68 [0.64–0.72]	0.44 ± 0.03	0.54 ± 0.03
Recovery cycle			
Refractoriness at 2.5 ms (%)	23.8 [13.4–34.2]	−4.8 ± 4.8	15.8 ± 12.3
Superexcitabilty (%)	**−26.2 [−28.2 to −24.2]**	**−37.5 ± 1.7**	**−32.4 ± 2.1**[†]
Late subexcitability (%)	13.9 [12.7–15.1]	11.8 ± 3.1	11.4 ± 0.9

Results in BVVL patients are expressed as mean ± standard error of the mean (SEM) and in healthy controls as mean and 95% confidence intervals (CI).
[†] *p*-Values comparing BVVL baseline to BVVL on riboflavin: [†] $p < 0.05$.

0.36–0.44), and rheobase (BVVL, 1.9 ± 1.1 mA; controls, 2.2 mA [95% CI 0.04–4.4]) were also similar.

A "fanned out" appearance of threshold electrotonus was evident in the BVVL patients, signifying greater threshold change to both depolarization and hyperpolarisation (Table 2, Fig. 1A). Specifically, TEd 90–100 ms (BVVL, 56.1 ± 2.3%; controls, 42.6% [95% CI 40.6–44.6]) and TEh 90–100 ms (BVVL, −151.7 ± 10.2%; controls, −107.8% [95% CI −116.6 to −99.0]) were significantly increased when compared to controls. The changes in TE were accompanied by abnormalities of the I/V gradient, whereby the resting I/V gradient was significantly reduced in BVVL patients (BVVL, 0.44 ± 0.03; controls, 0.68 [95% CI 0.64–0.72], Fig. 1B).

The recovery cycle of axonal excitability curves was markedly shifted downwards in BVVL patients when compared to controls (Fig. 1C). Specifically, there was a significant reduction in refractoriness at 2.5 ms (BVVL, −4.8 ± 4.8%; controls, 23.8 [95% CI 13.4–34.2]) and an increase in superexcitability (BVVL, −37.5 ± 1.7; controls, −26.2 [95% CI −28.2 to −24.2], Table 2, Fig. 1C) in subjects with BVVL. Late subexcitability was similar between the groups (BVVL, 11.8 ± 3.1; controls 13.9 [95% CI 12.7–15.1]).

3.3. Mathematical modeling of abnormal excitability properties

A mathematical model of the human motor axon was used to assist in interpreting the complex changes observed in

clinical nerve excitability. The model was initially adjusted to provide a close match to the age-matched control group and then used to explore whether changes in any membrane parameter could reproduce the changes seen in BVVL patient recordings (3 patients). Alterations in membrane conductances or potential in isolation could not account satisfactorily for the changes seen in subjects with BVVL. Membrane hyperpolarisation reduced the discrepancy by 67%, yet did not support similarities in late subexcitability, T_{SD} and threshold between BVVL patients and controls. Rather, increasing the Barrett and Barrett conductance (GBB) (see Section 6) from 35.2 to 50.5 units reduced the discrepancy by 76.7% (Fig. 2). The GBB refers to passive membrane property related to applied currents accessing and crossing the internodal compartment of the axon (Bostock et al., 1998). An increase in GBB may be caused by abnormal myelin permeability, secondary to thin or leaky myelin, or by a loosening of paranodal seal. Modeling of changes in two parameters improved the fit to 77.1% by means of increasing GBB from 35.2 to 47.5 units and reducing leak conductances from 1 to 0.82 units. Consequently, the mathematical modeling suggested that an increase in myelin permeability may account for the abnormalities of axonal excitability in BVVL, which is in keeping with previous findings that myelin maturation is accompanied by changes in the GBB (Farrar et al., 2013).
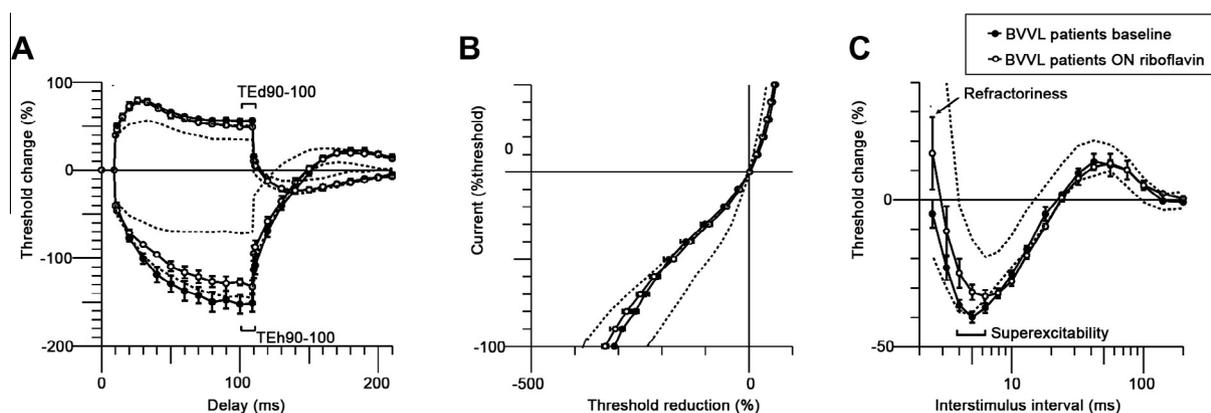
Fig. 1. Nerve excitability measures in BVVL patients and normal controls. Comparison of multiple measures of nerve excitability in median motor nerves in BVVL patients at baseline (filled circles) and normal controls (dashed lines) plotted as mean and standard errors of mean or 95% confidence intervals respectively. Riboflavin therapy resulted in significant modulation of excitability with partial reversibility of baseline changes (open circles = BVVL patients ON riboflavin therapy; filled circles = BVVL patients baseline). (A) Threshold electrotonus, depicting TEh 90–100 ms and TEd 90–100 ms. (B) Current threshold relationship. (C) Recovery cycle of excitability, demonstrating reduced refractoriness and increased superexcitability at baseline.
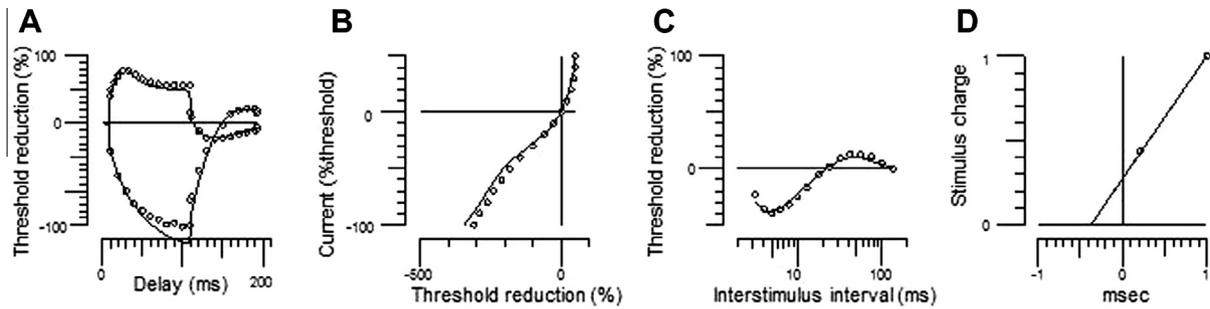
Fig. 2. Simulation of the excitability changes in clinical nerve excitability in BVVL patients using the mathematical model. Open circles represent the model generated by the normal control group. Black lines were generated by the model by increasing GBB from 35.2 units to 50.5 units, which reduced the discrepancy by 76.7%. (A) Threshold electrotonus for 100-ms polarizing currents ±40% of the resting threshold. (B) Current–threshold relationship. (C) Recovery cycles. (D) Charge–duration plot based on stimuli of 0.2 and 1 ms duration with the negative intercept on the *x*-axis equating to the strength–duration time constant, and the slope equal to the rheobase.

### 3.4. Assessments after 12 months of riboflavin

3.4.1. Improvement in motor nerve function

Treatment with riboflavin was accompanied by partial normalization of motor nerve function (Table 2, Fig. 1). Specifically, there was a significant improvement in threshold electrotonus, with reduced TEd (90–100 ms) and TEh (90–100 ms) (TEd 90–100 ms: $BVVL_{baseline}$, 56.1 ± 2.3, $BVVL_{on\ riboflavin}$, 49.3 ± 1.3, $p < 0.05$, TEh 90–100 ms: $BVVL_{baseline}$, −151.7 ± 10.2; $BVVL_{on\ riboflavin}$, −129.9 ± 5.5, $p < 0.05$). There was also an increase in resting I/V slope ($BVVL_{baseline}$, 0.44 ± 0.03; $BVVL_{on\ riboflavin}$, 0.54 ± 0.03, $p < 0.05$). Prominent changes were also noted in the recovery cycle of nerve excitability, with reduction in superexcitability ($BVVL_{baseline}$, −37.5 ± 1.7; $BVVL_{on\ riboflavin}$, −32.4 ± 2.1, $p < 0.05$) and an increase in refractoriness at 2.5 ms ($BVVL_{baseline}$, −4.8 ± 4.8; $BVVL_{on\ riboflavin}$, 15.8 ± 12.3, $p = 0.06$). The excitability changes suggested that riboflavin therapy exerted a stabilizing effect on myelin permeability in BVVL patients. There was also

an improvement in absolute scores for grip strength on dynamometry (Table 1), contrasting with the natural history outcomes in untreated BVVL patients, who typically experience progressive upper-limb weakness. This was paralleled by improvement on audiometry in the younger affected individuals (Fig. 3), and stable or improved respiratory function in all six individuals (Table 1).

4. Discussion

Utilizing the axonal excitability technique, the present study indicates that abnormalities of passive membrane properties were a feature of BVVL. Specifically, an increase in depolarizing and hyperpolarizing threshold electrotonus, termed the 'fanned-out' appearance, was evident in BVVL. The changes in TE were accompanied by a reduction in the current–threshold slope and refractoriness, along with an increase in superexcitability. Mathematical modeling suggested that abnormalities of axonal excitability were best explained by alteration in passive membrane
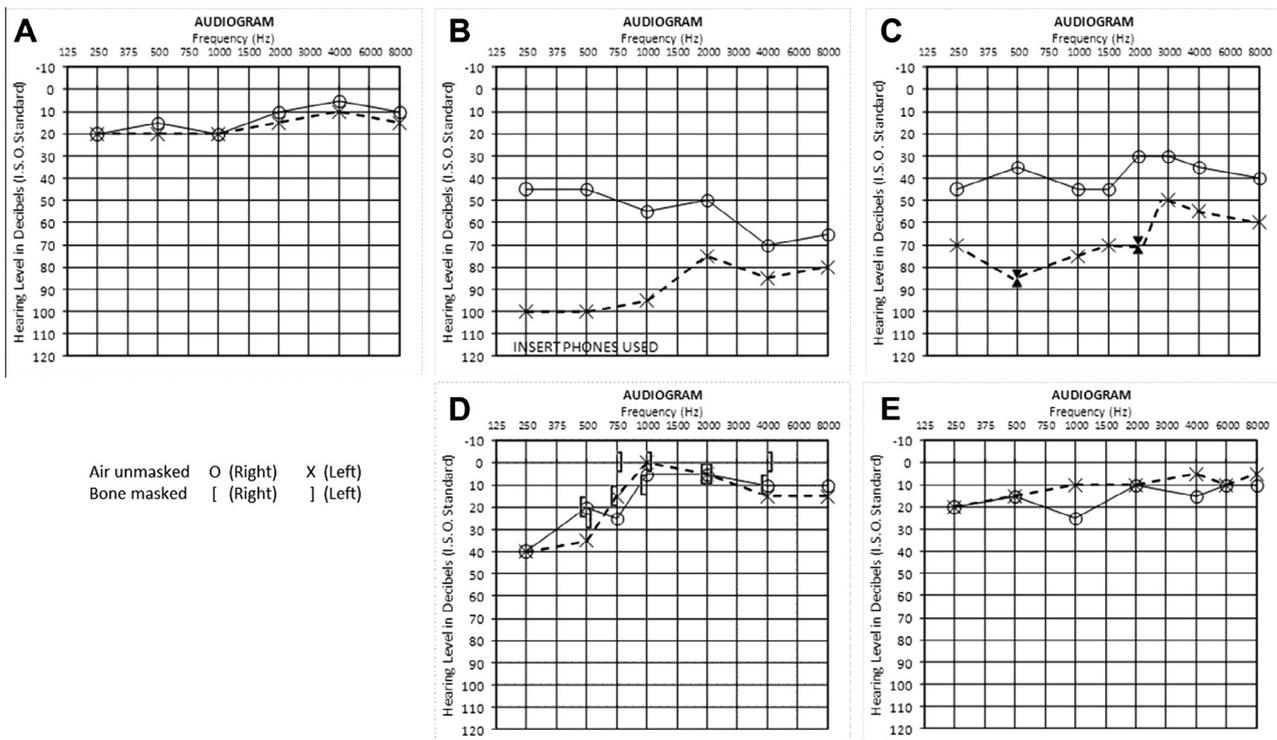
Fig. 3. Audiometry in BVVL patients before and after riboflavin therapy. Audiometry in patient 1.2 (A, B, C) and 1.1 (D, E) showing deterioration during disease course, and improvement following riboflavin therapy. Patient 1.2 progressed from normal (A) to severe hearing loss (B) over 12 months with improvement after 12 months of riboflavin therapy (C). Patient 1.1 was diagnosed with low frequency hearing loss at baseline (D) that returned to normal after 12 months of riboflavin therapy (E).

properties, namely an increase in the Barrett and Barrett conductance (GBB), while axonal ion channel function and resting membrane potential were maintained. Importantly, the increase in GBB could be attributed to an increase in myelin permeability, either due to thin or leaky myelin or an increased permeability of the paranodal region, a pathophysiological process that may be secondary to riboflavin deficiency.

4.1. Pathophysiological mechanisms underlying BVVL neuropathy

Although riboflavin deficiency secondary to *SLC52A2* gene mutation is postulated to underlie the BVVL phenotype, the pathophysiological processes mediating this condition remain to be fully elucidated. Importantly, BVVL is characterized by a sensorimotor axonal neuropathy (Foley et al., 2014). Given the riboflavin is an important co-factor in the synthesis of myelin (Champe et al., 2008), it could be hypothesized that abnormalities of myelin permeability may account for the development of the BVVL neuropathy. Schwann cells are critical in maintaining axonal integrity, and axonal degeneration due to primary Schwann cell and myelin dysfunction has been demonstrated in other inherited neuropathies (Sahenk, 1999; Nave et al., 2007; Scherer and Wrabetz, 2008; Beirowski, 2013).

Importantly, myelin adheres to axons at the paranodal junction, an axonal region that is permeable to small molecules, thereby forming a pathway to 'short-circuit' the nodal currents (Rosenbluth et al., 2013). Of relevance, the paranodal currents may traverse three possible pathways including along the paranodal periaxonal space, the obliquely oriented transverse bands and between adjacent lamellae of myelin sheaths (Mierzwa et al., 2010). While structural changes in peripheral nerve myelination have not been previously described in BVVL, the findings in the present study would suggest dysfunction at the paranodal region, particularly loosening of the paranodal seal, may lead to an increase in GBB and superexcitability. The changes demonstrated here are due to functional alteration in the myelin (increased permeability), rather than demyelination. Consequently, significant changes in motor conduction velocity would not be expected, a notion underscored by the nerve conduction study findings in the BVVL cohort (Table 1). Further, it should be highlighted that the axonal excitability abnormalities evident in BVVL are different from those previously described in maturing nerves (Nodera et al., 2004; Farrar et al., 2013, 2014), thereby arguing against the possibility that the present findings relate simply to delayed nerve maturation. Underscoring this notion are pathological studies in riboflavin deficient animal models, which develop a similar neuropathy to BVVL patients, disclosing abnormalities of myelin with dissociation of both the inner and outer spirals of the myelin lamellae (Norton et al., 1976; Jortner et al., 1987). In a mouse model of mitochondrial dysfunction, cerebroside depletion was shown to interfere with the maintenance of Schwann cell-axon contacts on electron microscopic analysis, with enlarged nodal gaps and axons that had pulled away from their myelin sheaths (Viader et al., 2013).

It could be argued that age was a confounding factor in the present study, particularly given that GBB changes with nerve maturation. This seems an unlikely given that an age-matched reference model was used and that maturational changes in axonal excitability reach a plateau in adolescence (8–15 years), the very age of two of the patients modeled (1.1 and 1.2). Separately, it may be expected that an increase in GBB should also lead to reduction in T_{SD}, although this was not observed in the current study. T_{SD} depends on many membrane parameters and a possible explanation may relate to subtle differences in these (for example leak conductance, nodal capacitance, nodal K^+ and Na^+ conductances or nodal width) (Bostock, 1983). This notion is supported by the mathematical simulations of excitability changes in the present study, as a reduction in leak conductance should lead to an increase in T_{SD}, opposing the effect of increasing GBB.

4.2. Progress with riboflavin therapy

The natural history of BVVL is of progressive neurodegeneration together with decline in motor amplitudes (Foley et al., 2014) Previous excitability studies in motor neuron disease have demonstrated progressive axonal dysfunction paralleling clinical impairment and established the reproducibility of axonal excitability (Farrar et al., 2011; Cheah et al., 2012). Consequently the longitudinal improvement in nerve excitability profiles with riboflavin treatment in all BVVL patients in this series appears incongruous with the natural history suggesting that riboflavin exerts a positive effect on peripheral nerve function with modulation of myelin dysfunction. This is likely to be operating at a molecular and biochemical level, with improvements in Schwann cell energy supply and myelin synthesis. Stabilization of the myelin sheath would in turn be expected to prevent further axonal degeneration and promote recovery, which is supported by the motor amplitudes remaining stable. In our cohort, following therapy with riboflavin, the established and severe sensory neuronopathy did not improve with therapy. In contrast, neuropathy of more recent onset (motor neuropathy of onset in late 1st decade and mild in the younger siblings, VIII nerve involvement hearing loss in the younger children) improved significantly with therapy. This emphasizes the need for clinicians to diagnose and commence therapy early in children with the disorder.

5. Conclusion

Taken together, findings from the present study suggest that an increase in myelin permeability at the paranode is a feature of BVVL, which may be partially normalized with riboflavin therapy. These findings also suggest that nerve excitability studies may be further developed in larger cohorts as a potential biomarker, to identify and monitor treatment response, and to guide more specific and tailored treatment strategies for BVVL patients.

6. Glossary

Accommodation half time

A parameter measured during 40% depolarizing threshold electrotonus obtained as the time threshold reduction returned to half way between the peak and plateau levels.

Electrotonus

Changes in membrane potential evoked by subthreshold depolarizing or hyperpolarizing current pulses.

'Fanning out'

A term to illustrate alterations in threshold electrotonus waveforms associated with their resemblance to a Japanese fan, specifically the curves shift curves outwards with greater threshold changes.

Hyperpolarization

The membrane potential becomes more negative. This occurs following tetanisation of release of ischemia.

Membrane potential

Voltage change across the axonal membrane (inside–outside).

Relative refractory period (RRP)

The phase between the end of the absolute refractory period and the beginning of the superexcitable period, when the threshold is increased due to inactivation of transient Na^+ channels.

Rheobase

The least current amplitude of infinite duration that attains threshold.

Late subexcitability

The period of reduced excitability following the superexcitability period during the recovery cycle of excitability. It is measured as the largest mean increase in threshold in 3 adjacent points (peak) and is a biomarker of nodal K^+ channel conduction.

Superexcitability

An increase in excitability that occurs shortly after a nerve impulse and a biomarker of paranodal fast K^+ channel conduction. It is measured as the mean percentage reduction in threshold of the three lowest (peak) adjacent points during the recovery cycle of excitability.

T_{SD}

Strength duration time constant (T_{SD}) describes the rate at which threshold current increases as stimulus width is reduced and is calculated using Weiss' formula. T_{SD} is a nodal property, partially dependent on persistent Na^+ conductances and also the passive membrane time constant (the product of resting resistance and nodal capacitance).

Threshold (current)

The stimulus current required to evoke a compound potential that was 40% of the maximum.

Threshold electrotonus (TE)

Threshold changes produced by prolonged subthreshold depolarizing or hyperpolarizing currents to modify the potential difference through the internodal axonal membrane. TE provides information about internodal membrane properties and conductances, in addition to an estimate of resting membrane potential.

Acknowledgements

References

Beirowski B. Concepts for regulation of axon integrity by enwrapping glia. Front Cell Neurosci 2013;7:256.

Bosch AM, Abeling NG, Ijlst L, Knoester H, van der Pol WL, Stroomer AE, et al. Brown–Vialetto–Van Laere and Fazio Londe syndrome is associated with a riboflavin transporter defect mimicking mild MADD: a new inborn error of metabolism with potential treatment. J Inherit Metab Dis 2011;34:159–64.

Bostock H. The strength–duration relationship for excitation of myelinated nerve: computed dependence on membrane parameters. J Physiol 1983;341:59–74.

Bostock H, Baker M, Reid G. Changes in excitability of human motor axons underlying post-ischaemic fasciculations: evidence for two stable states. J Physiol 1991;441:537–57.

Bostock H, Cikurel K, Burke D. Threshold tracking techniques in the study of human peripheral nerve. Muscle Nerve 1998;21:137–58.

Champe PC, Harvey RA, Ferrier DR. Complex lipid metabolism. In: Champe PC, Harvey RA, editors. Lippincott's illustrated reviews: biochemistry. 4th ed. Philadelphia: Lippincott Williams & Wilkins; 2008. p. 201–18.

Cheah BC, Lin CS, Park SB, Vucic S, Krishnan AV, Kiernan MC. Progressive axonal dysfunction and clinical impairment in amyotrophic lateral sclerosis. Clin Neurophysiol 2012;123:2460–7.

Farrar MA, Park SB, Krishnan AV, Kiernan MC, Lin CS. Axonal dysfunction, dysmyelination and conduction failure in HNPP. Muscle Nerve 2014;49:858–65.

Farrar MA, Park SB, Lin CS, Kiernan MC. Evolution of peripheral nerve function in humans: novel insights from motor nerve excitability. J Physiol 2013;591:273–86.

Farrar MA, Vucic S, Lin CS, Park SB, Johnston HM, du Sart D, et al. Dysfunction of axonal membrane conductances in adolescents and young adults with spinal muscular atrophy. Brain 2011;134:3185–97.

Foley AR, Menezes MP, Pandraud A, Gonzalez MA, Al-Odaib A, Abrams AJ, et al. Treatable childhood neuronopathy caused by mutations in riboflavin transporter RFVT2. Brain 2014;137:44–56.

Francis DA, Ponsford JR, Wiles CM, Thomas PK, Duchen LW. Brown–Vialetto–Van Laere syndrome. Neuropathol Appl Neurobiol 1993;19:91–4.

Green P, Wiseman M, Crow YJ, Houlden H, Riphagen S, Lin JP, et al. Brown–Vialetto–Van Laere syndrome, a ponto-bulbar palsy with deafness, is caused by mutations in c20orf54. Am J Hum Genet 2010;86:485–9.

Haack TB, Makowski C, Yao Y, Graf E, Hempel M, Wieland T, et al. Impaired riboflavin transport due to missense mutations in SLC52A2 causes Brown–Vialetto–Van Laere syndrome. J Inherit Metab Dis 2012;35:943–8.

Johnson JO, Gibbs JR, Megarbane A, Urtizberea JA, Hernandez DG, Foley AR, et al. Exome sequencing reveals riboflavin transporter mutations as a cause of motor neuron disease. Brain 2012;135:2875–82.

Jortner BS, Cherry J, Lidsky TI, Manetto C, Shell L. Peripheral neuropathy of dietary riboflavin deficiency in chickens. J Neuropathol Exp Neurol 1987;46:544–55.

Kiernan MC, Burke D, Andersen KV, Bostock H. Multiple measures of axonal excitability: a new approach in clinical testing. Muscle Nerve 2000;23:399–409.

Kiernan MC, Mogyoros I, Burke D. Differences in the recovery of excitability in sensory and motor axons of human median nerve. Brain 1996;119:1099–105.

Mierzwa A, Shroff S, Rosenbluth J. Permeability of the paranodal junction of myelinated nerve fibers. J Neurosci 2010;30:15962–8.

Nave KA, Sereda MW, Ehrenreich H. Mechanisms of disease: inherited demyelinating neuropathies – from basic to clinical research. Nat Clin Pract Neurol 2007;3:453–64.

Nodera H, Bostock H, Kuwabara S, Sakamoto T, Asanuma K, Jia-Ying S, et al. Nerve excitability properties in Charcot-Marie-Tooth disease type 1A. Brain 2004;127:203–11.

Norton WN, Daskal I, Savage HE, Seibert RA, Lane M. Effects of riboflavin deficiency on the ultrastructure of rat sciatic nerve fibers. Am J Pathol 1976;85:651–60.

Preston DC, Shapiro BE. Electromyography and neuromuscular disorders: clinical-electrophysiologic correlations. 3rd ed. Elsevier Health Sciences; 2012.

Rosenbluth J, Mierzwa A, Shroff S. Molecular architecture of myelinated nerve fibers: leaky paranodal junctions and paranodal dysmyelination. Neuroscientist 2013;19:629–41.

M.P. Menezes et al./Clinical Neurophysiology xxx (2015) xxx–xxx

Sahenk Z. Abnormal Schwann cell–axon interactions in CMT neuropathies. The effects of mutant Schwann cells on the axonal cytoskeleton and regeneration-associated myelination. Ann N Y Acad Sci 1999;883:415–26.

Sathasivam S. Brown–Vialetto–Van Laere syndrome. Orphanet J Rare Dis 2008;3:9.

Scherer SS, Wrabetz L. Molecular mechanisms of inherited demyelinating neuropathies. Glia 2008;56:1578–89.

Viader A, Sasaki Y, Kim S, Strickland A, Workman CS, Yang K, et al. Aberrant Schwann cell lipid metabolism linked to mitochondrial deficits leads to axon degeneration and neuropathy. Neuron 2013;77:886–98.

Vucic S, Kiernan MC. Axonal excitability properties in amyotrophic lateral sclerosis. Clin Neurophysiol 2006;117:1458–66.

Vucic S, Kiernan MC. Abnormalities in cortical and peripheral excitability in flail arm variant amyotrophic lateral sclerosis. J Neurol Neurosurg Psychiatry 2007a;78:849–52.

Vucic S, Kiernan MC. Pathophysiologic insights into motor axonal function in Kennedy disease. Neurology 2007b;69:1828–35.

Yao Y, Yonezawa A, Yoshimatsu H, Masuda S, Katsura T, Inui K-i. Identification and comparative functional characterization of a new human riboflavin transporter hRFT3 expressed in the brain1-3. J Nutr 2010;140:1220–6.